Turning-induced surface integrity for a fillet radius in a 316L austenitic stainless steel

Maxime Dumas, Guillaume Kermouche, Frédéric Valiorgue, Alexis van Robaeys, Fabien Lefebvre, Alexandre Brosse, Habib Karaouni, Joël Rech

Version of Record: https://www.sciencedirect.com/science/article/pii/S1526612521003613
Manuscript_c03e90a8b3bb95391ab08694f6382f31

Turning-induced surface integrity for a fillet radius in a 316L austenitic stainless steel

May 13, 2021

Maxime DUMAS

Univ. Lyon, ENISE, LTDS, UMR CNRS 5513, 58 rue Jean Parot, 42000 Saint Etienne, France

Airbus Helicopters, Aéroport Marseille Provence, 13725 Marignane, France

E-mail : maxime.dumas@enise.fr

Guillaume KERMOUCHE *Mines Saint-Etienne, CNRS, UMR 5307 LGF, Centre SMS, F-42023 Saint Etienne, France*

E-mail : kermouche@emse.fr

Frédéric VALIORGUE *Université de Lyon, Ecole Nationale d'Ingénieurs de Saint Etienne, LTDS UMR CNRS 5513, 58 rue Jean Parot, 42100 Saint Etienne, France*

E-mail : frederic.valiorgue@enise.fr

Alexis VAN ROBAEYS *Airbus Helicopters, Aéroport Marseille Provence, 13725 Marignane, France*

E-mail : alexis.van-robaeys@airbus.com

Fabien LEFEBVRE *Cetim, 52 Avenue Félix Louat, 60304 Senlis, France*

E-mail : fabien.lefebvre@cetim.fr

Alexandre BROSSE *Framatome, 10 Rue Juliette Récamier, 69456 Lyon, France*

E-mail : alexandre.brosse@framatome.com

Habib KARAOUNI *Safran Tech, Rue des Jeunes-Bois, 78772 Magny-les-Hameaux, France*

E-mail : habib.karaouni@safrangroup.com

Joel RECH *Université de Lyon, Ecole Nationale d'Ingénieurs de Saint Etienne, LTDS UMR CNRS 5513, 58 rue Jean Parot, 42100 Saint Etienne, France*

E-mail : joel.rech@enise.fr

Highlights

- For the first time, turning-induced surface integrity in a 316L is studied along a fillet radius.
- Turning-induced affected depth depends on the angular position in the fillet radius.
- The affected depth is twice larger for longitudinal turning than for face turning.
- The microstructure evolution is correlated with the average uncut chip thickness parameter and the cutting edge radius.
- Severe plastic deformation at room temperature or/and at high strain rate governs microstructural evolution (occurrence of deformation twinning).

Graphical abstract

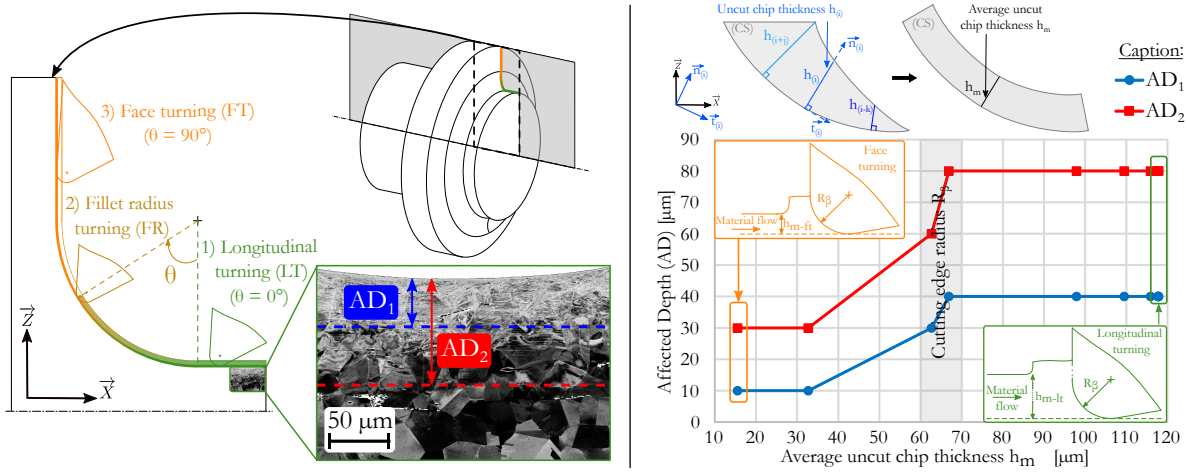

Abstract

Turning is a machining process extensively applied to produce revolution parts. Durability of these parts are known to depend on the turning process signature that is often referred as surface integrity. The surface integrity generated in a fillet radius has been barely studied in the literature so far, despite the well-known geometrical stress concentration factor of such singularities. Therefore this paper deals with the investigation of machining-induced surface integrity when turning a fillet radius in a 316L austenitic stainless steel. Different characterization methods are used for that purpose - SEM, EBSD, nanoindentation and X-Ray diffraction. It points out that the turning-induced consequences are not homogeneous along the machined profile. Residual stresses are strongly affected and microstructure is highly modified over a depth of 80 μm that leads to a mechanical properties gradient. It is evidenced that the average uncut chip thickness is the main governing parameter regarding surface integrity. It is also reported that deformation twins appear in the affected zone. It highlights that turning-induced microstructure

evolution at a given depth is rather a consequence of severe plastic deformation at high strain rate than dynamic recrystallization.

Keywords: fillet radius; turning; microstructure modifications; residual stresses; average uncut chip thickness; deformation twinning

1 Introduction

In-service life of industrial critical components does strongly depend on functional surfaces that result from surface manufacturing processes. Machining processes and more precisely turning are common process to finish functional parts. The extensive development in turning has made this kind of processes able to reach micron-size precisions in terms of surface topology. However machining remains a mechanical process. Therefore, like most surface mechanical treatments, it also leads to in-depth material modifications - up to a few hundred of microns for some specific cases [1]. These induced modifications - microstructure, residual stresses - are usually gathered in the embedding concept of surface integrity [2, 3]. For most of surface mechanical treatments respectively based on impacts [4] or low-plasticity sliding contact [5], significant enhancement of fatigue life or wear resistance have been reported, mostly because of the high level of induced compressive stresses or of surface hardening resulting from in-depth microstructure gradient [6]. On the contrary, machining processes involve high-friction and significant temperature rise over a few tens of microns that can lead in some cases to tensile stresses, phase transformations or some microstructural defects in the near-surface [7]. A thin white layer composed of ultrafine grains is commonly induced by turning operation. It is assumed to be a consequence of dynamic recrystallization phenomena [8, 9]. Below this thin layer, an hardened zone is usually observed that can be related to dynamic recovery. Therefore high in-depth microstructural and mechanical gradients usually result from turning operation that is clearly a major issue regarding the durability of engineering parts, especially fatigue life [10, 11].

A significant attention has been paid in the past ten years to the prediction of turning-induced surface integrity through coupled experimental-computationnal approaches for various materials [12, 13]. The relation between turning-induced surface integrity and fatigue life was also explored recently [14]. It evidenced that both topography and residual stress field play on the number of cycles to failure. Nonetheless, it must be noted that most of these investigations remained limited to the restrictive assumptions of orthogonal cutting or longitudinal cutting. Regarding fatigue life, there is clearly a lack of knowledge concerning the turning induced surface integrity in geometrical singularities, such as fillet radii, that are known to promote fatigue crack nucleation and propagation due to geometrically-induced stress concentration [15]. A preliminary investigation from the authors of this paper was performed on a 15-5PH martensitic stainless steel [16]. It highlighted a change in residual stress field along the fillet radius but

with almost no microstructure or hardness modifications. This was explained by the small grain size of the 15-5PH martensitic structure and low strain hardening modulus that prevents microstructure modifications to be observed. Hence it is important to get first experimental insights about the surface-integrity modifications when turning a fillet radius in a medium grain-sized material that also exhibits high strain hardening ability.

This paper thus focuses on a 316L austenitic steel, for which extensive efforts have been done to evidence induced residual stresses whether after orthogonal cutting [17] or longitudinal turning [12, 18, 19]. On the contrary, turning-induced microstructure modifications in 316L has been less explored so far, except the papers of Zhang et al. and Chang et al. that characterized the microstructure modifications induced by a milling operation [1, 20]. Most of investigations have dealt with other manufacturing processes such as Rotationally Accelerated Shot Peening [21], Surface Mechanical Rolling Treatment [5], Equal Channel Angular Pressing [22], High Pressure Torsion [23], or in the framework of mechanical testing such as Split Hopkinson Pressure bar (hat-shaped specimen) [24], tensile tests [25] or combined torsion and tension tests [26]. Like residual stress-field, microstructure features may also play a significant role regarding surface durability, especially if stress-corrosion is the expected failure mode [20].

This paper aims at investigating the surface integrity of a 316L austenitic steel when turning a fillet radius. The first part deals with materials and process descriptions and characterization methods employed to highlight surface integrity modifications. Results are then presented in terms of affected depth along the fillet radius for both residual stress and microstructure modifications. Eventually, the last section discusses the surface integrity modification mechanisms at stake in 316L in relation with the varying geometrical cutting parameters along the fillet radius.

2 Material and methods

The case-study is described in Fig 1. Three different zones can be distinguished : the longitudinal turning, the fillet radius turning and the face turning (from the part axis to the outer surface) respectively named hereafter as LT Zone, FR Zone and FT zone. A rhombic DNMG 150608 PM 1525 insert (nose radius R_ϵ = 0.8 mm, cutting edge radius R_β = 70 μm) in a PDJNL 2020 K15 tool holder (cutting edge angle κ_r = 93°) is used. Cutting conditions are summarized in Tab. 1.

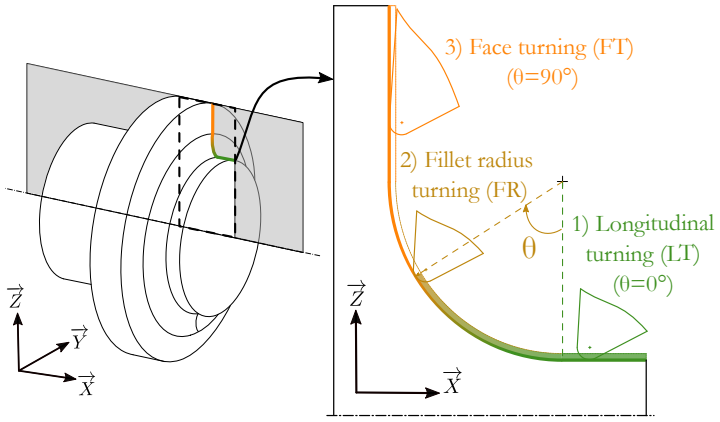

Fig. 1: Case-study: the fillet radius turning. Given a turned workpiece, a cross-section is extracted perpendicular to the cutting speed. The angle coordinate θ enables to locate the tool along the machined profile. Three areas are distinguished : 1) longitudinal turning (LT) (θ=0°, length=2.5mm), 2) fillet radius turning (FR) (radius=5mm) and 3) face turning (FT) (θ=90°, length=5mm). This already evidences that the cutting regime varies along the fillet radius.

Table 1: Cutting conditions

Cutting speed *Vc*	**Feed *f***	**Depth of cut *ap***	**Lubrication**
[m.min^{-1}]	[mm.rev^{-1}]	[mm]	-
100	0.3	0.3	Dry cutting

The 316L steel chemical composition is given in Tab. 2. MnS inclusions are observed parallel to the rolling direction (Fig 2). These inclusions are likely due to the high percentage of Sulphur (0.027%) in the used material. The mean grain size lies between 20 and 50 μm. One can notice the presence of annealing twins in the bulk microstructure.

Table 2: 316L chemical composition in %wt

C	**Si**	**Mn**	**Ni**	**Cr**	**Mo**	**Cu**	**S**
0.018	0.444	1.276	10.168	16.764	2.026	0.365	0.027

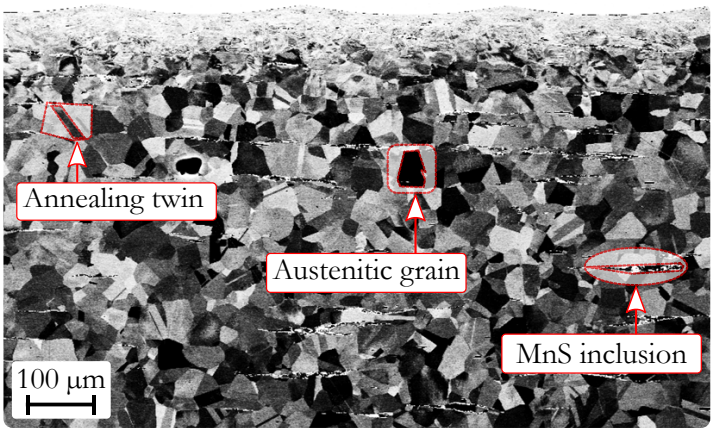

Fig. 2: Microstructure of the 316L austenitic stainless steel higlighted by Scanning Electron Microscopy (Back-Scattering mode). It reveals austenitic grains with a size between 20 and 50 μm, annealing twins induced by the manufacturing process and M_nS inclusions due to a high percentage of sulpher in the studied material.

Microstructure observations to quantify grain size, turning affected zones and metallurgical transformations are performed using a Zeiss® Supra55V Scanning Electron Microscope in BackScattering mode (20 KeV). Cross-sections are prepared perpendicular to the cutting direction. Samples are extracted from the workpiece by mean of Wire Electrical Discharge Machining. They are then coated with a Nickel layer to protect the outer surface during mechanical polishing. EBSD measurements are achieved with a 60 nm step size on specific areas of 60x120 μm in dimensions. It allows Inverse Pole Figure (IPF) mapping of the grain orientations and computing Kernel Average Misorientation (KAM) map to highlight turning-induced in-depth strain hardening. Let us note that EBSD indexation rate in the very near surface, often called Tribologically Transformed Layer by [27] or White Layer by [28], is quite low due to friction-induced severe plastic deformation and grain refinement. Therefore white pixels in EBSD maps are those for which the indexation failed.

Nano-indentation grids (60x120 μm) are also carried out to evidence modifications of mechanical properties induced by the machining operation using a DCM nanoidentation Set Up (MTS®) which allows the use of Continuous Stiffness Method [29]. The penetration depth is set to 300 nm and space between indents is about 5 μm. The results are mapped in 2D using TriDiMap toolbox so as to relate the hardness values to microstructural features [30].

Microstructural observations (60x120 μm) are conducted at four different positions (at the bottom of machining streaks) along the machined profile: LT zone, 65° in FR zone that will be referred as FR65, 80° in FR zone that will be referred as FR80 and FT zone as shown in Fig 1.

Residual stresses induced by the turning operation are analyzed by X-Ray Diffraction using a PROTO® set-up. They are run in two directions: the feed direction and the cutting direction. The experimental setting are detailed by Valiorgue et al [12]. Note that contrary to the microstructural and mechanical measurements, residual stress profiles were only measured on LT and FT zones due to accessibility issues in the fillet radius.

3 Results

The turning process is known to induce large microstructure modifications beneath the machined surface. The thermomechanical contact between the tool and the workpiece can lead in the 316L steel to intra-grain orientation gradients, slip bands, twinning-induced plasticity, grain refinement or phase transformations [23]. It is proposed in this paper to define three different *Affected Depth (**AD**)* to quantify the mechanically affected thickness as illustrated in Fig 3 from microstructural observations. AD_0 corresponds to the near surface that is composed of submicrometric grains. AD_1 is characterized by severely deformed grains that appear as grains with a high density of slip bands. The criterion used to measure the length of AD_1 is that 100% of the grains at a given depth exhibit a significant density of slip bands. AD_2 is the whole mechanically affected depth. As a consequence, the length of AD_2 is defined as the depth below which no more slip bands induced by turning are observed over a given cross-section. These parameters are measured in the fillet radius for different values of angle coordinate θ defined in Fig 1. Up to the knowledge of authors, it is the first time that slip bands are used to quantify machining-induced affected depth. It is worth noting that such a methodology might be easily embedded in a semi-automatic digital approach to assess microstructural surface integrity [31].

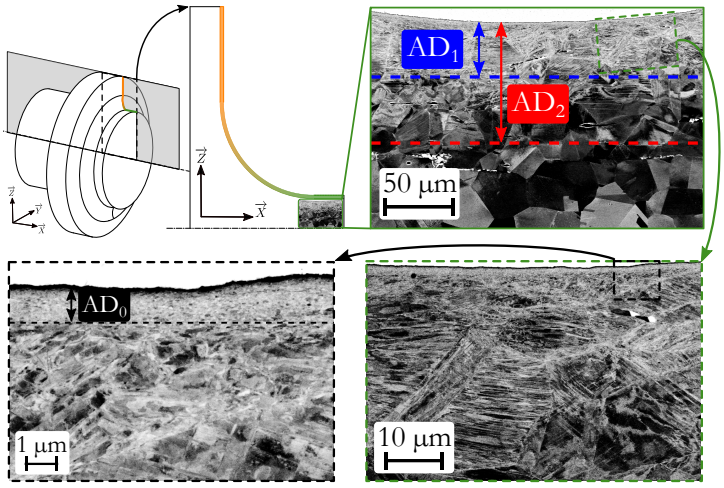

Fig. 3: Turning-induced microstructure gradient beneath the surface in the case of longitudinal turning assessed by SEM (Back-Scattering mode). The first layer AD_0 includes submicrometric grains, the second layer AD_1 is composed of severely deformed grains and the third one AD_2 represents the whole affected depth below which no more slip bands are visible.

Therefore microstructure evolution along the fillet radius is highlighted in Fig 4. It can be observed that AD_0 is around 1 μm. As its evolution is not significant with regard to the measuring uncertainty, it can not be analyzed further. Fig 4 shows the evolution of AD_1 and AD_2 as a function of the angle coordinate θ in the fillet radius. AD_1 and AD_2 remain constant (40 μm and 80 μm respectively) until $\theta = 70°$. Then it starts decreasing until the face turning configuration is reached with respective values about 10 μm and 30 μm. It is assumed that a change in local cutting conditions may be responsible. This point will be discussed later in the paper.

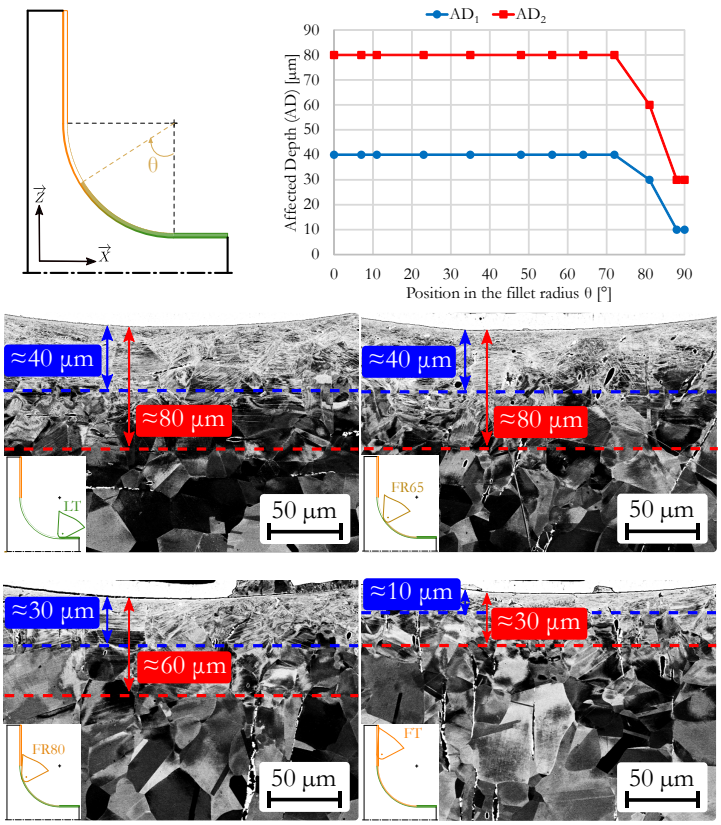

Fig. 4: Evolution of the turning-induced microstructure gradient modifications for several angle coordinates θ in the fillet radius. Four positions are highlighted: LT (θ=0°), FR65 (θ=65°), FR80 (θ=80°) and FT (θ=90°). The affected depth remains constant until the position of 70° in the radius. Then it reduces up to face turning.

Fig 5 shows the evolution of nanoindentation hardness beneath the surface. The global trend is a decrease in hardness in terms of affected depth along the machined profile. Some local maximum appear which correspond whether to the presence of MnS inclusions or highly deformed grains. Similarly to SEM observations, the turning affected zone seems to be smaller in the FT zone than in the LT zone. Hardness gradient is almost similar for LT zone and FR65 zone. It starts decreasing for FR80 zone. The change in mechanical properties seems to be well correlated to microstructure modifications highlighted in Fig 4.

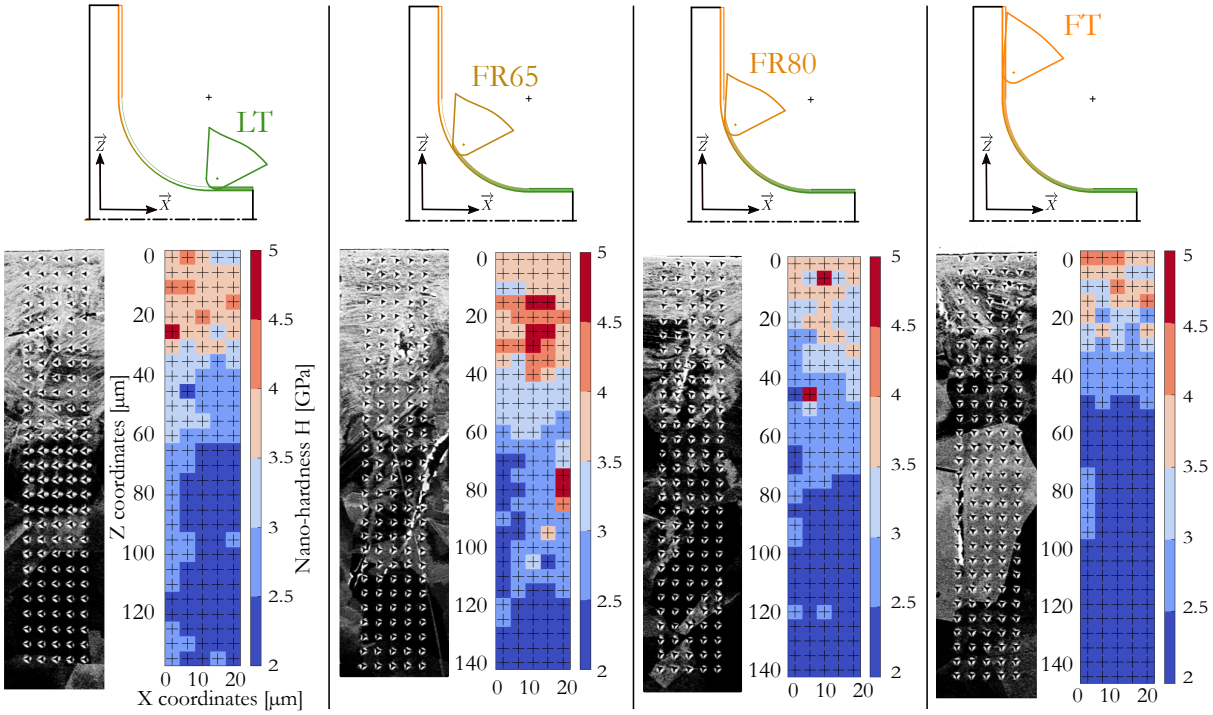

Fig. 5: Hardness maps beneath the surface characterized by Nanoindentation testing for four positions: LT (θ=0°), FR65 (θ=65°), FR80 (θ=80°) and FT (θ=90°). The hardness gradients are closed for LT et FR65 positions but the affected depth starts reducing from FR80. Some local maximum appear due to MnS inclusions and severely deformed grains.

EBSD measurements are also performed on LT and FT areas. A decreasing intra-grain misorientation is observed which is here also consistent with surface strain hardening induced by mechanical contacts [27]. Fig 6 highlights that the AD_1 depth is approximately twice thicker in longitudinal turning than in face turning, as observed with SEM (Fig 4). It also points out the presence of deformation twins in some grains inside the AD_2 region in the case of longitudinal turning. Deformation twinning is not observed in face turning. However indexation quality is relatively poor in the severely deformed zone that likely prevent deformation twins to be observed by EBSD. One may note that deformation twins lead to a local increase in nanoindentation hardness. M'Saoubi and Ryde also early used the EBSD technique to evidence the induced plasticity in austenitic chip material when performing orthogonal cutting [32]. Moreover, Zhang et al. recently used the same technique to assess the machining-induced microstructure alteration and plastic deformation during a milling operation [1].

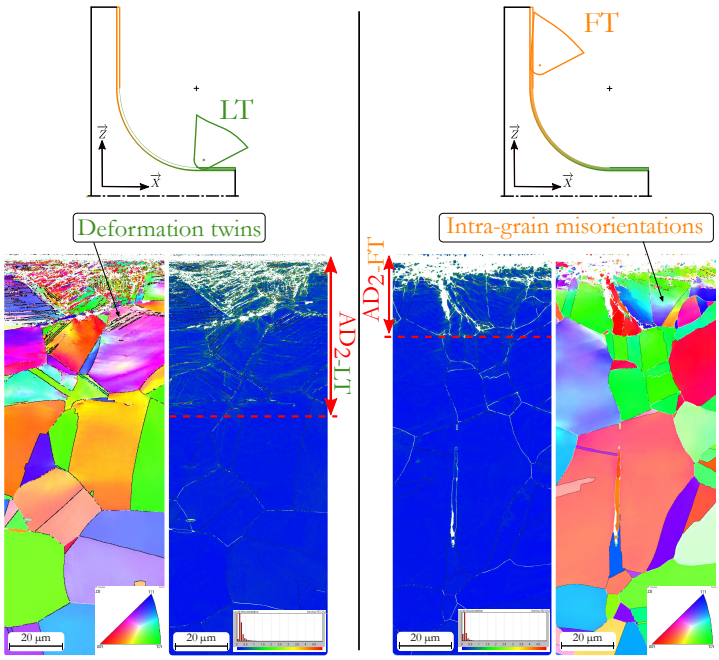

Fig. 6: Turning-induced microstucture modifications characterized by EBSD in the case of longitudinal turning LT and face turning FT. Inverse Pole Figures Z evidence grains refinement, intra-grain misorientations and deformation twins. Kernel Average Misorientation maps reveal that the affected depth is approximately twice thicker in the case of longitudinal turning AD_{2-LT} than in face turning AD_{2-FT}.

Fig 7 shows that the residual stress profiles have a typical machining-induced hook-shape, as already commented by M'Saoubi et al. [33], for both LT and FT zones. The first 20 μm exhibit important tensile stresses for the two cases and in the two considered directions. The affected depth is twice smaller and the compression peak is significantly lower for face turning. One may notice small oscillations of the face-turning residual stress profiles when approaching the zero-stress state. This is likely a consequence of the electropolishing procedure or some other second-order measurement artefacts. The results are similar to those communicated by Valiorgue et al. [12]. One can note that the maximum residual tensile stress is always higher for the cutting direction. Full Width at Half Maximum of the diffraction peak is often used as a qualitative measurement of strain hardening and dislocation density even though exact quantification would require a refined analysis of the diffraction peak [34]. From FWHM, it might be concluded that the machined 316L is less strain hardened in the case of face turning than in the case of longitudinal turning (approximately 25 μm compared to 75 to 100 μm) that is also consistent with nanohardness and EBSD-SEM measurements.

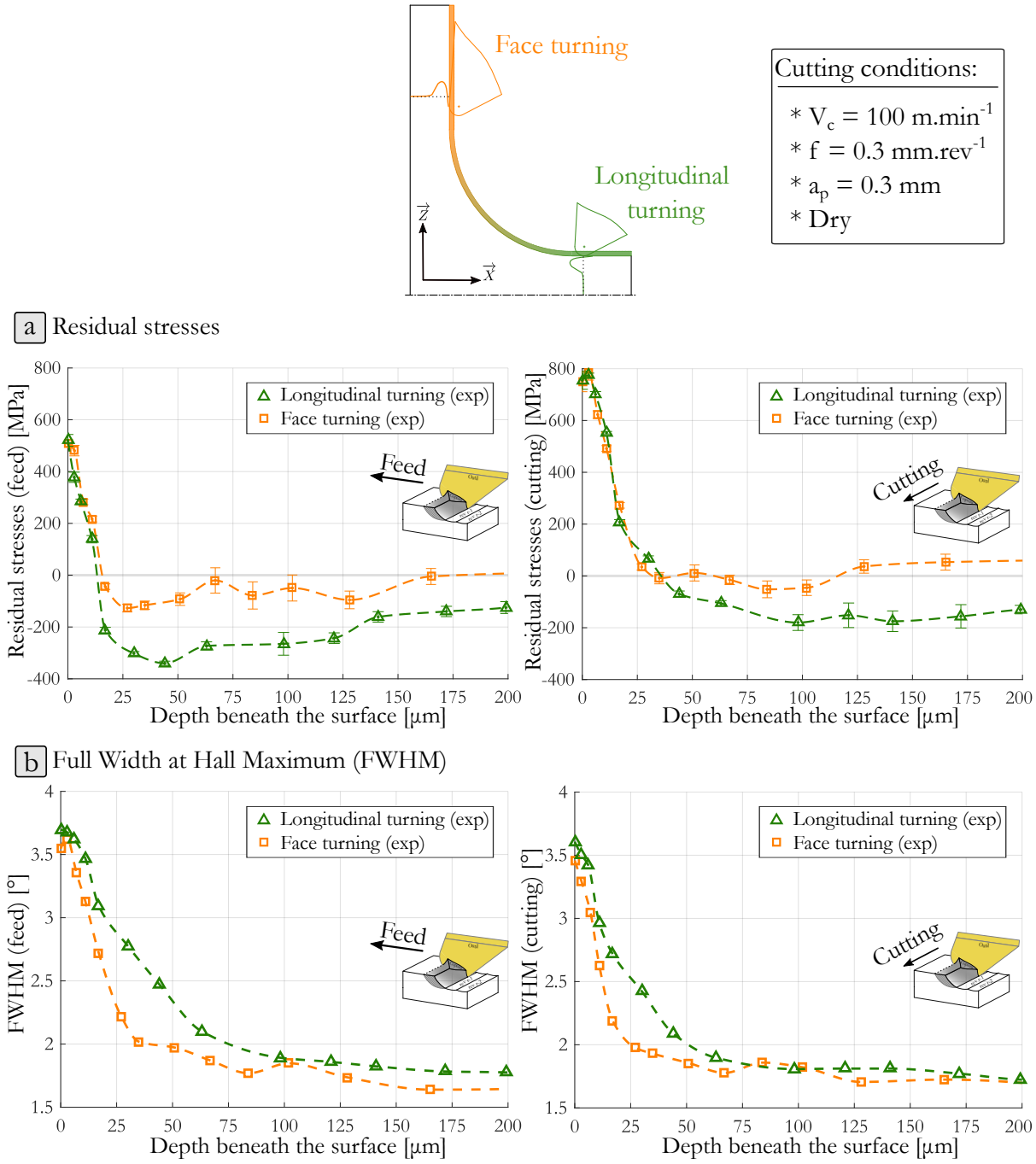

Fig. 7: a) comparison of the turning-induced residual stresses analyzed by X-Ray diffraction in two directions for LT (triangle markers) and FT (square markers) zones. Both residual stress profiles start with a tensile-twenty-microns layer and differ then in terms of compression peak intensity and affected depth. b) analysis of FWHM in longitudinal turning and face turning cases. It qualitatively concludes to a higher in-depth hardening for LT than for FT

4 Discussion

This paper clearly highlights the effect of cutting conditions on near-surface turning-induced microstructural and mechanical modifications. The hardening gradient depth is of the same order of magnitude

using different characterization methods - nanoindentation (hardness), X-Ray Diffraction (FHWM), SEM (Slip-Bands) and EBSD (misorientations) whatever the position in the fillet radius. Turning clearly affects microstructure over a larger depth than the well-known microstructure-modified outer surface, often named white layer. This is in opposition with the recent results on a 15-5PH martensitic stainless steel that reported no variation in microstructure evolution along the fillet radius radius [16]. In this study, the main difference is the small size ($\approx 1\ \mu m$) of the martensitic needles compared to the 316L austenitic grains ($\approx 50\ \mu m$), that prevents observation of slip-bands and intra-grain disorientation. Moreover 316L steel is known to much more strain-harden than 15-5PH that makes nanoindentation more sensitive to microstructure evolution.

The affected depth is shown to be dependent on the position in the fillet radius. Face turning leads to a lower in-depth hardening gradient than longitudinal turning. The corresponding affected depth remains similar in the fillet radius until the angular position reaches 70°. This is likely a consequence of a change in local cutting conditions. To illustrate this, let us consider a local cutting parameter used by many authors in the case of orthogonal cutting: the uncut chip thickness h [17, 35] (Fig 8-b). It corresponds to the thickness of the theoretical section to be cut (CS), that is to say a rectangle in such a case and consequently h is equal to the tool feed. However, when considering a real 3D turning operation (Fig 8-a), the theoretical cut section is no more rectangular and has a shape depending on tool geometry and cutting conditions, especially feed cutting and depth of cut. As a consequence, it seems relevant to take into account these phenomena with the notion of average uncut chip thickness h_m. This geometrical parameter represents the average thickness of the cut section distributed along the cutting edge, as defined in Fig 8. Given a cutting edge geometry, h_m can be computed through eq (1).

$$h_m = \frac{1}{p}\sum_{i=1}^{p} h_{(i)} \tag{1}$$

where h_m is the average uncut chip thickness, $h_{(i)}$ is the uncut chip thickness in the $\overrightarrow{n_{(i)}}$ direction for a given angular position in the cutting edge geometry, p is the number of point to consider. Fig 9 plots the evolution of AD_1 and AD_2 as a function of h_m. The average uncut chip thickness (resp. affected depth) in case of face turning is more than 7 times (resp. 4 times) lower than in longitudinal turning. When the average uncut chip thickness is higher: 60-70 μm, the affected depth remains constant whereas it decreases accordingly to h_m once below. It is worth noting that the cutting edge radius value is close to this range. Therefore there might be a strong correlation between affected depth and cutting edge radius R_β.

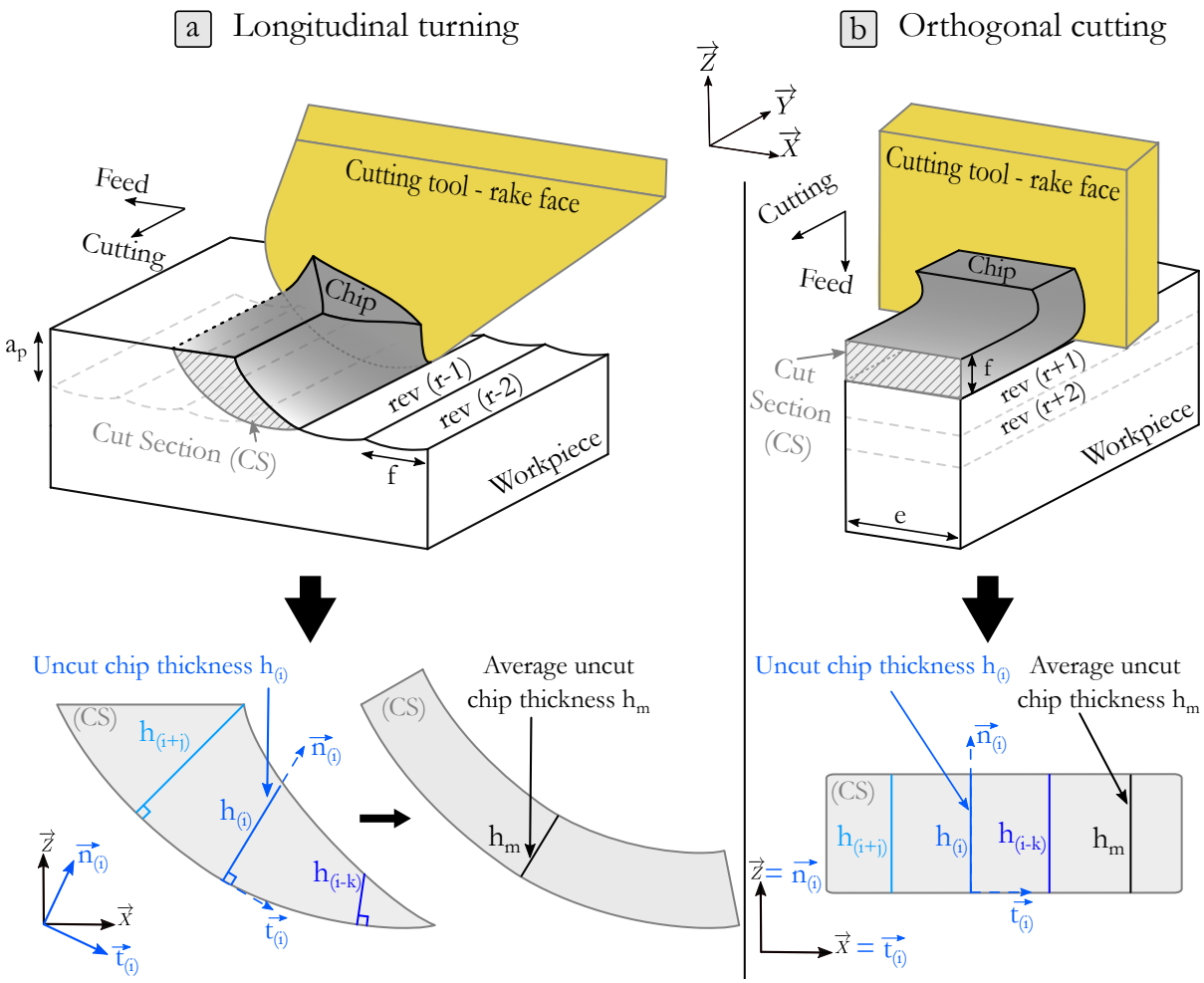

Fig. 8: Definition of the average uncut chip thickness h_m in a) longitudinal turning contrary to the uncut chip thickness h in b) orthogonal cutting. h_m corresponds to the average thickness of the theoretical section distributed along the cutting edge.

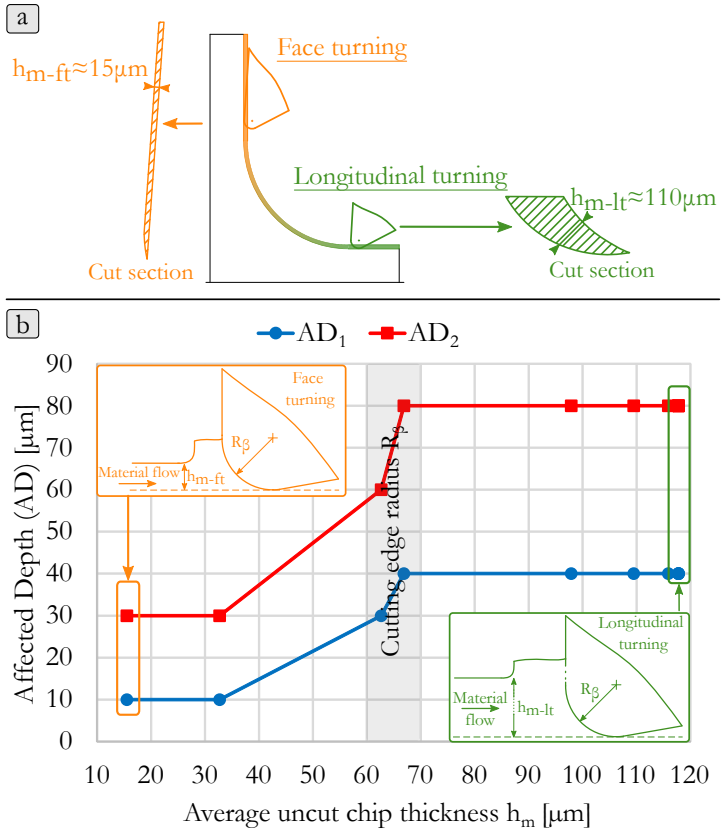

Fig. 9: a) illustration of the cut sections with the corresponding average uncut chip thickness h_m in LT and FT cases. In LT configuration, h_m is approximately 7 times higher than in LT. b) evolution of the affected depths AD_1 and AD_2 as a function of the average uncut chip thickness h_m. A threshold effect is observed for h_m higher than the cutting edge radius value: 60-70 μm (angular coordinate of 70°). The affected depths decrease below this value.

The severely deformed AD_1 region is composed of grains with high density of slip bands and deformation twins. In most of investigations dealing with microstructure evolution in austenitic stainless steels, deformation twins appear as a consequence of severe plastic deformation at low temperature [23], which is intrinsically related to the low stacking fault energy of such materials [36]. Deformation twining can also occur at high temperature but under high strain rate [37]. More precisely, it appears that high strain rate is required to avoid dynamic recovery or recrystallisation to happen. Therefore the occurrence of deformation twinning in turning is whether a consequence of cold deformation in the near-surface or to very high strain rate at high temperature [38]. It is worth noting that Zhang et al. reported slip bands but seemingly no deformation twins after a milling operation on a 316L steel [1]. No deformation twins are observed in face turning in the present paper. Deformation twinning is thus a consequence of severe cutting conditions that lead to subsurface severe plastic deformation under very high strain rate. Discontinuous dynamic recrystallization would unlikely appear in this zone since the time-scale might not be consistent with grain nucleation and grain boundary migration mechanisms [39].

In the very-near surface, the AD_0 zone is typical of a Tribologically Transformed Layer (commonly referred as a White Layer) already observed after milling of a 316L austenitic stainless steel [1, 20],

after orthogonal cutting of a Nickel-based superalloy [8] or longitudinal turning of a 15-5PH martensitic stainless steel [16]. This layer is likely a consequence of severe plastic deformation and high temperature induced by the friction between the tool and the workpiece. It can be assumed that dynamic/static recrystallization happens in this region that can leads sometimes to a near-surface softening/hardening as highlighted out by Liao et al. [8] or Kermouche et al. [40] using high speed friction tests on Copper. The mechanism leading to the creation of this zone requires a very good knowledge of the thermomechanical path over a few microns and an extensive use of advanced characterization methods at the white layer scale [8]. Finite Element Models might be useful to extract plastic stain, plastic strain rate and temperature for each layer beneath the surface to perform a deeper analysis of the deformation mechanisms observed experimentally. For instance, Jacquet et al. performed such analysis regarding the friction-induced microstructure in Copper and have concluded on the importance of discontinuous dynamic and post-dynamic recrystallisation mechanisms on the resulting near-surface microstructure [41]. It is thus beyond the scope of the present paper.

X-Ray diffraction (Fig 7) reveals that the depth over which residual stresses is non-zero in longitudinal and face turning is larger than the depth of the hardening gradient. This has been observed by number of authors working on surface mechanical treatments. For instance, similar results were reported by Zhou et al. with shot peening and Surface Mechanical Attrition Treatment (SMAT) [6]. Residual stress is mostly a consequence of plastic strain incompatibilities that induce residual elastic strain below the affected plastic zone whereas hardening is the consequence of the total plastic strain [42]. For both longitudinal and face turning, significant tensile stresses are observed over the first 20 microns. Then it turns into compressive stresses over 100-200 microns with a significant higher amplitude for longitudinal turning. Computation of fatigue life at high number of cycles (HCF) should predict that face turning is more detrimental to durability. In the framework of low cycle fatigue (LCF), both residual stress and hardening play a role. Compressive stresses prevent crack to propagate but material hardening can be detrimental to durability by enhancing stress relaxation. To conclude on fatigue life, it will be necessary to run fatigue tests and consider the effect of surface topography on fatigue crack initiation that will be the goal of future paper.

5 Conclusions

The turning-induced surface integrity when turning a fillet radius in a 316L austenitic stainless steel has been studied using various microstructural and mechanical characterization methods. The main conclusions can be drawn as follows:

- The affected depth in terms of microstructure and mechanical property modifications is twice larger for longitudinal turning than for face turning.
- Deformation twins appear in longitudinal turning. It highlights that microstructural evolution

mechanisms are governed by severe plastic deformation at room temperature or/and at high strain rate.

- The residual stress profiles differ in terms of compression peak and affected depth between longitudinal turning and face turning.
- Turning affected depth in terms of microstructure modifications depends on the angular position in the fillet radius. A threshold effect appears below an angular coordinate of 70°.
- The microstructure evolution is correlated with the average uncut chip thickness parameter h_m. The affected depth remains stable until h_m reaches the cutting edge radius value, then it decreases.

Acknowledgments

Authors are thankful to Airbus Helicopters, Safran Tech, Framatome and Cetim for their financial support. Authors would also acknowledge M.Cici, H.Pascal from ENISE and M.Mondon from EMSE for their valuable support regarding the machining of sample, XRD analysis and SEM/EBSD observations. Eventually, authors would thank Claire Maurice and Emeric Plancher for helpful discussions.

References

[1] Zhang W, Wang X, Hu Y, Wang S. Quantitative studies of machining-induced microstructure alteration and plastic deformation in aisi 316 stainless steel using ebsd. Journal of Materials Engineering and Performance. 2018;27(2):434–446. doi:10.1007/s11665-018-3129-9.

[2] Rech J, Hamdi H, Valette S. Workpiece surface integrity. in: Davim J.P (Ed.), Machining-Fundamentals and Recent advances. Springer London, 2008. Ch. 3. pp. 59–96. doi:10.1007/978-1-84800-213-5.

[3] Jawahir I.S, Brinksmeier E, M'Saoubi R, Aspinwall D.K, Outeiro J.C, Meyer D, Umbrello D, Jayal A.D. Surface integrity in material removal processes: Recent advances. CIRP Annals. 2011;60(2):603–626. doi:10.1016/j.cirp.2011.05.002.

[4] Ueno H, Kakihata K, Kaneko Y, Hashimoto S, Vinogradov A. Enhanced fatigue properties of nanostructured austenitic sus 316l stainless steel. Acta Materialia. 2011;59(18):7060–7069. doi:10.1016/j.actamat.2011.07.061.

[5] Huang H.W, Wang Z.B, Lu J, Lu K. Fatigue behaviors of aisi 316l stainless steel with a gradient nanostructured surface layer. Acta Materialia. 2015;87:150–160. doi:10.1016/j.actamat.2014.12.057.

[6] Zhou J, Retraint D, Sun Z, Kanouté P. Comparative study of the effects of surface mechanical attrition treatment and conventional shot peening on low cycle fatigue of a 316L stainless steel. Surface and Coatings Technology. 2018;349:556–566. doi:10.1016/j.surfcoat.2018.06.041.

[7] M'Saoubi R, Axinte D, Herbert C, Hardy M, Salmon P. Surface integrity of nickel-based alloys subjected to severe plastic deformation by abusive drilling. CIRP Annals. 2014;63(1):61–64. doi:10.1016/j.cirp.2014.03.067.

[8] Liao Z, Polyakov M, Diaz O.G, Axinte D, Mohanty G, Maeder X, Michler J, Hardy M. Grain refinement mechanism of nickel-based superalloy by severe plastic deformation - Mechanical machining case. Acta Materialia. 2019;180:2–14. doi:10.1016/j.actamat.2019.08.059.

[9] Mondelin A, Valiorgue F, Rech J, Coret M, Feulvarch E. Modeling of surface dynamic recrystallisation during the finish turning of the 15-5ph steel. Procedia CIRP. 2013;8:311–315. doi:10.1016/j.procir.2013.06.108.

[10] Javidi A, Rieger U, Eichlseder W. The effect of machining on the surface integrity and fatigue life. International Journal of Fatigue. 2008;30(10-11):2050–2055. doi:10.1016/j.ijfatigue.2008.01.005.

[11] M'Saoubi R, Outeiro J.C, Chandrasekaran H, Dillon Jr O.W, Jawahir I.S. A review of surface integrity in machining and its impact on functional performance and life of machined products. International Journal of Sustainable Manufacturing. 2008;1(1/2):203. doi:10.1504/IJSM.2008.019234.

[12] Valiorgue F, Rech J, Hamdi H, Gilles P, Bergheau J.M. 3d modeling of residual stresses induced in finish turning of an aisi 304l stainless steel. International Journal of Machine Tools and Manufacture. 2012;53(1):77–90. doi:10.1016/j.ijmachtools.2011.09.011.

[13] Mondelin A, Valiorgue F, Rech J, Coret M, Feulvarch E. Hybrid model for the prediction of residual stresses induced by 15-5ph steel turning. International Journal of Mechanical Sciences. 2012;58(1):69–85. doi:10.1016/j.ijmecsci.2012.03.003.

[14] Chomienne V, Verdu C, Rech J, Valiorgue F. Influence of surface integrity of 15-5ph on the fatigue life. Procedia Engineering. 2013;66:274–281. doi:10.1016/j.proeng.2013.12.082.

[15] Pilkey W.D, Peterson R.E. Peterson's Stress Concentration Factors. 2nd Edition. Wiley, 1997.

[16] Dumas M, Valiorgue F, Kermouche G, Robaeys A.V, Masciantonio U, Brosse A, Karaouni H, Rech J. Evolution of the surface integrity while turning a fillet radius in a martensitic stainless steel 15-5PH. Procedia CIRP. 2020;87:101–106. doi:10.1016/j.procir.2020.02.038.

[17] Outeiro J.C, Umbrello D, M'Saoubi R. Experimental and numerical modelling of the residual stresses induced in orthogonal cutting of AISI 316L steel. International Journal of Machine Tools and Manufacture. 2006;46(14):1786–1794. doi:10.1016/j.ijmachtools.2005.11.013.

[18] Outeiro J.C, Dias A.M, Jawahir I.S. On the effects of residual stresses induced by coated and uncoated cutting tools with finite edge radii in turning operations. CIRP Annals. 2006;55(1):111–116. doi:10.1016/S0007-8506(07)60378-3.

[19] Leppert T, Peng R.L. Residual stresses in surface layer after dry and mql turning of aisi 316l steel. Production Engineering. 2012;6(4-5):367–374. doi:10.1007/s11740-012-0389-3.

[20] Chang L, Burke M.G, Scenini F. Stress corrosion crack initiation in machined type 316l austenitic stainless steel in simulated pressurized water reactor primary water. Corrosion Science. 2018;138:54–65. doi:10.1016/j.corsci.2018.04.003.

[21] Li J.S, Gao W.D, Cao Y, Huang Z.W, Gao B, Mao Q.Z, Li Y.S. Microstructures and mechanical properties of a gradient nanostructured 316l stainless steel processed by rotationally accelerated shot peening. Advanced Engineering Materials. 2018;20(10):1800402. doi:10.1002/adem.201800402.

[22] Ueno H, Kakihata K, Kaneko Y, Hashimoto S, Vinogradov A. Nanostructurization assisted by twinning during equal channel angular pressing of metastable 316L stainless steel. Journal of Materials Science. 2011;46(12):4276–4283. doi:10.1007/s10853-011-5303-4.

[23] Scheriau S, Zhang Z, Kleber S, Pippan R. Deformation mechanisms of a modified 316l austenitic steel subjected to high pressure torsion. Materials Science and Engineering: A. 2011;528(6):2776–2786. doi:10.1016/j.msea.2010.12.023.

[24] Xue Q, Liao X.Z, Zhu Y.T, Gray G.T. Formation mechanisms of nanostructures in stainless steel during high-strain-rate severe plastic deformation. Materials Science and Engineering: A. 2005;410-411:252–256. doi:10.1016/j.msea.2005.08.022.

[25] Wu X, Pan X, Mabon J.C, Li M, Stubbins J.F. The role of deformation mechanisms in flow localization of 316l stainless steel. Journal of Nuclear Materials. 2006;356(1-3):70–77. doi:10.1016/j.jnucmat.2006.05.047.

[26] Zhang J, Huang Z, Rui W, Li J, Tian Y, Li J. Effect of combined torsion and tension on the microstructure and fracture behavior of 316l austenitic stainless steel. Journal of Materials Engineering and Performance. 2019;28(9):5691–5701. doi:10.1007/s11665-019-04316-4.

[27] Tumbajoy-Spinel D, Descartes S, Bergheau J.M, Lacaille V, Guillonneau G, Michler J, Kermouche G. Assessment of mechanical property gradients after impact-based surface treatment: Application to pure α-iron. Materials Science and Engineering: A. 2016;667:189–198. doi:10.1016/j.msea.2016.04.059.

[28] Rech J, Moisan A. Surface integrity in finish hard turning of case-hardened steels. International Journal of Machine Tools and Manufacture. 2003;43(5):543–550. doi:10.1016/S0890-6955(02)00141-4.

[29] Guillonneau G, Kermouche G, Bec S, Loubet J.L. A simple method to minimize displacement measurement uncertainties using dynamic nanoindentation testing. Tribology International. 2014;70:190–198. doi:10.1016/j.triboint.2013.10.013.

[30] Mercier D. Tridimap toolbox (2014).
URL https://tridimap.readthedocs.io/en/latest/getting_started.html

[31] la Monaca A, Liao Z, Axinte D. A digital approach to automatically assess the machining-induced microstructural surface integrity. Journal of Materials Processing Technology. 2020;282:116703. doi:10.1016/j.jmatprotec.2020.116703.

[32] M'Saoubi R, Ryde L. Application of the ebsd technique for the characterisation of deformation zones in metal cutting. Materials Science and Engineering: A. 2005;405(1-2):339–349. doi:10.1016/j.msea.2005.06.002.

[33] M'Saoubi R, Outeiro J.C, Changeux B, Lebrun J.L, Morão Dias A. Residual stress analysis in orthogonal machining of standard and resulfurized aisi 316l steels. Journal of Materials Processing Technology. 1999;96(1-3):225–233. doi:10.1016/S0924-0136(99)00359-3.

[34] Borbély A, Ungár T. X-ray line profiles analysis of plastically deformed metals. Comptes Rendus Physique. 2012;13(3):293–306. doi:10.1016/j.crhy.2011.12.004.

[35] Nasr M.N.A, Ng E.G, Elbestawi M.A. Modelling the effects of tool-edge radius on residual stresses when orthogonal cutting aisi 316l. International Journal of Machine Tools and Manufacture. 2007;47(2):401–411. doi:10.1016/j.ijmachtools.2006.03.004.

[36] Sakai T, Belyakov A, Kaibyshev R, Miura H, Jonas J.J. Dynamic and post-dynamic recrystallization under hot, cold and severe plastic deformation conditions. Progress in Materials Science. 2014;60:130–207. doi:10.1016/j.pmatsci.2013.09.002.

[37] Yapici G.G, Karaman I, Luo Z.P, Maier H.J, Chumlyakov Y.I. Microstructural refinement and deformation twinning during severe plastic deformation of 316L stainless steel at high temperatures. Journal of Materials Research. 2004;19(8):2268–2278. doi:10.1557/JMR.2004.0289.

[38] Zhu Y.T, Liao X.Z, Wu X.L. Deformation twinning in nanocrystalline materials. Progress in Materials Science. 2012;57(1):1–62. doi:10.1016/j.pmatsci.2011.05.001.

[39] Piot D, Smagghe G, Jonas J.J, Desrayaud C, Montheillet F, Perrin G, Montouchet A, Kermouche G. A semitopological mean-field model of discontinuous dynamic recrystallization: Toward a correct and rapid prediction of grain-size distribution. Journal of Materials Science. 2018;53(11):8554–8566. doi:10.1007/s10853-018-2137-3.

[40] Kermouche G, Jacquet G, Courbon C, Rech J, Zhang Y.Y, Chromik R. Microstructure evolution induced by sliding-based surface thermomechanical treatments - application to pure copper. Materials Science Forum. 2016;879:915–920. doi:10.4028/www.scientific.net/MSF.879.915.

[41] Jacquet G, Kermouche G, Courbon C, Tumbajoy D, Rech J. Effect of sliding velocity on friction-induced microstructural evolution in copper. IOP Conference Series: Materials Science and Engineering. 2014;63:012039. doi:10.1088/1757-899X/63/1/012039.

[42] Zhou J, Sun Z, Kanouté P, Retraint D. Reconstruction of residual stress and work hardening and their effects on the mechanical behaviour of a shot peened structure. Mechanics of Materials. 2018;127:100–111. doi:10.1016/j.mechmat.2018.09.005.